

DETERMINING THE SPATIAL COHERENCE OF TURBULENCE AT MHK SITES

Levi F. Kilcher*

National Renewable Energy Laboratory
Golden, Colorado, USA

Jim Thomson

NNMREC
University of Washington
Seattle, Washington, USA

Jonathan Colby

Verdant Power
New York, New York, USA

ABSTRACT

Although turbulence is thought to be a key variable in the performance and survivability of Marine Hydrokinetic turbines, it has not been fully characterized at sites where they will be deployed. In particular, the conventional metrics of turbulence intensity and turbulent kinetic energy spectra only describe the turbulence at a point. Spatial information is required to estimate the loading across a rotor, for example, and to understand the short-term evolution of turbulence in the vicinity of a device (for potential use in feed-forward control algorithms). Here, we describe a method to collect and analyze data for determining the spatial coherence of turbulence at marine hydrokinetic turbine deployment sites. The approach uses multiple compliant moorings equipped with acoustic Doppler velocimeters and inertial motion units. Analysis of data from previous deployments of a single mooring is used to demonstrate the method, and future deployments are discussed. It is expected that coherence will be highly dependent on scale, with high coherence for large-scale eddies, and low coherence for the smaller, inertial-scale eddies.

1 INTRODUCTION

The marine and hydrokinetic (MHK) turbine industry needs accurate estimates of fatigue loading in order to meet device-lifetime goals. Accurate fatigue-load estimates (e.g. using Hydro-FAST or Tidal BladedTM) require accurate knowledge of the turbulent inflow environment. In particular, comprehensive turbulence datasets at tidal, river and ocean-current sites are needed. Critical statistics of these datasets include: mean shear, the turbulent kinetic energy (TKE) spectrum, Reynold's stresses, and spatial coherence (i.e., length scales) of turbulent eddies (Figure 1).

Experience from the wind industry has shown that these variables play a role in determining device fatigue loads and performance [1–3]. Mean shear can induce variable loads on the device rotor as it rotates through a non-uniform velocity profile. The TKE spectrum and Reynold's stresses quantify the size, amplitude and orientation of turbulent eddies that can interact with a blade or the entire rotor. Spatial coherence - an indicator of the length (l) of eddies as a function of their diameter (d , Figure 1) - is important because longer eddies are likely to induce larger fatigue loads on turbines. An eddy that hits the entire blade, for example, will induce a larger load on that blade than an eddy of equal amplitude and shorter length.

The first three of these variables have been well quantified using low-cost measurement techniques. The mean shear and Reynold's stress can be estimated from bottom-mounted Acoustic Doppler Profiler (ADP) measurements [4, 5]. The TKE spectrum can be measured using moored acoustic Doppler velocimeters (ADV) that are equipped with inertial motion sensors [6]. Here we compare spatial coherence estimates from a fixed-frame ADV deployment with those from a compliant-mooring ADV deployment and describe a test deployment to improve and extend the moored approach.

2 STUDY SITES AND METHODS

The primary dataset used in this work was collected at the Admiralty Head site (Figure 2, yellow). The water-depth at this site is approximately 55m deep and is located 500m southwest of Admiralty Head. The data was collected from a compliant 'Tidal Turbulence Mooring' (hereafter TTM) with ADVs mounted 10, 11 and 14m above the seafloor. These heights were chosen to match the intended hub-heights of turbines planned for the site. The ADV at 11m was equipped with a MicroStrain 3DM-GX3-25 inertial motion sensor (IMU) that recorded ADV orientation

*Corresponding Author: levi.kilcher@nrel.gov

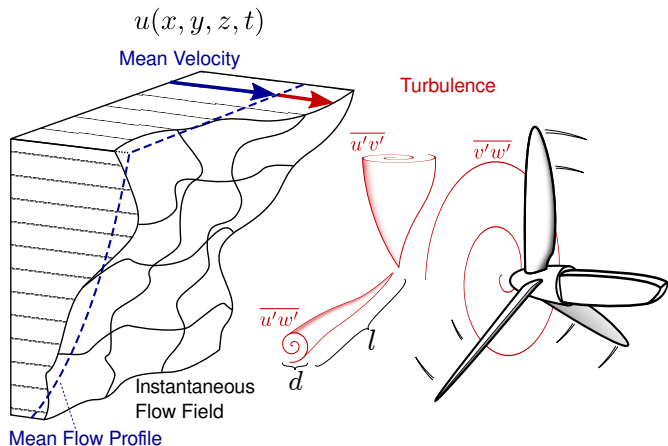


FIGURE 1. SCHEMATIC OF AN MHK TURBINE IN A TURBULENT FLOW FIELD. THE TURBULENCE (RED) IS SUPERIMPOSED ON THE MEAN VELOCITY PROFILE (BLUE). EDDIES IN DIFFERENT ORIENTATIONS CONTRIBUTE TO DIFFERENT COMPONENTS OF THE REYNOLD'S STRESS ($\overline{u'w'}$, $\overline{v'w'}$, $\overline{w'w'}$). THE ENERGY, SIZE (d) AND LENGTH (l) OF THESE EDDIES ARE IMPORTANT TO TURBINE FATIGUE LOADING.

and all 6 degrees of motion (3 rotation, 3 translational) synchronous with each velocity measurement [8]. The other two ADVs were equipped with ‘quasi-synchronous’ X-IO Technologies x-IMUs. Where, quasi-synchronous means that the independent time-stamps of the IMU and ADV can be used to sync those measurements to within a few seconds.

This work only utilizes the ADVs at 10 and 11m. The Microstrain-equipped ADV at 11m was on the same rigid vane (strongback) as the 10m ADV. Lagged cross-correlations of these instruments \vec{u} were used to synchronize the two instrument’s measurements to within 0.1seconds throughout the 2-day deployment. This facilitated interpolation of the Microstrain’s motion signals onto the 10m ADV timeseries so that time-domain motion correction (next section) could be performed on that ADV’s timeseries as well.

This dataset also includes velocity profile measurements from an upward-looking Nortek Acoustic Wave and Current profiler (AWAC) mounted on the mooring anchor. For periods up to several hours, the TTM was in the path of one of the AWAC’s acoustic beams and the AWAC velocity measurements were contaminated by side-lobe reflection from the mooring. These periods were screened from the AWAC measurements using signal-amplitude thresholds.

Thomson et.al. (2013) showed that mooring motion can effectively be removed from the TKE spectrum using quasi-synchronous IMU measurements and ‘spectral motion correction’ methods. This work demonstrates that moored synchronous IMU-ADV measurements can be used to remove mooring mo-

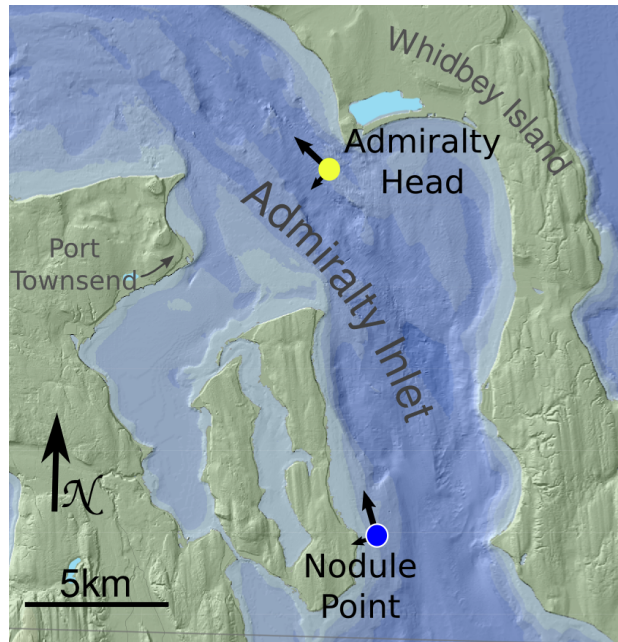


FIGURE 2. MAP OF ADMIRALTY INLET INDICATING LOCATIONS OF THE NODULE POINT (BLUE) AND ADMIRALTY HEAD (YELLOW) MEASUREMENT SITES [7]. STREAM-WISE AND CROSS-STREAM PRINCIPAL AXES DIRECTIONS ARE INDICATED BY LARGE AND SMALL ARROWS, RESPECTIVELY, AT EACH DOT.

tion in the time-domain and that this provides a framework for estimating coherence from moored ADV measurements. The time-domain method is preferred, because it retains higher-order properties of the flow, rather than just the variance spectrum (i.e., the TKE spectrum).

This work also utilizes turbulence measurements from two other measurement campaigns: 1) the ‘Nodule Point’ site in Admiralty Inlet (Figure 2, blue), and 2) the Verdant Power RITE site in New York City’s East River. At the ‘Nodule Point’ site in Admiralty Inlet (Figure 2, blue), an ADV was mounted on a fixed frame 4.6m above the seabed [4]. At the RITE site, two ADVs were mounted on a tower 4.6m above the seafloor and separated laterally by 0.5m [9].

2.1 Motion Correction

ADV on mooring lines change orientation and measure a velocity signal that is contaminated by the mooring’s motion. The orientation and motion resolved by tightly synchronized (with the ADV measurements) low-noise, low-bias IMUs can be used to correct for these effects in post-processing,

$$\vec{u}(t) = \vec{u}_{ADV}(t) + \vec{u}_m(t) \quad . \quad (1)$$

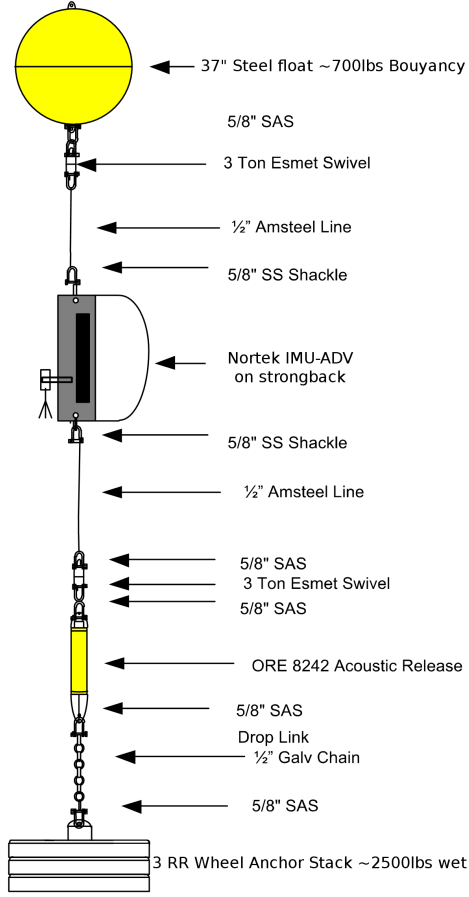


FIGURE 3. A SCHEMATIC OF A TTM WITH ONE ‘STRONG-BACK’ VANE THAT ORIENTS AN ADV INTO THE FLOW. A TTM CAN BE CONFIGURED WITH MULTIPLE STRONGBACKS WITH UP TO TWO ADVS, OR OTHER INSTRUMENTS, ON EACH.

Here ‘ \sim ’ denotes a quantity in the instrument-frame, \vec{u}_{ADV} is the uncorrected (raw) ADV velocity signal and \vec{u}_m is the ADV sensor’s motion. Note that the sign of \vec{u}_m in (1) is correct because the motion-induced velocity measured by the ADV is opposite its motion. \vec{u}_m is computed from the IMU rotation rate vector ($\vec{\omega}$) and linear-acceleration (\vec{a}) as,

$$\vec{u}_m(t) = \vec{\omega}(t) \times \vec{\ell} + \int \vec{a}'(t) dt \quad , \quad (2)$$

where $\vec{\ell}$ is the vector from the IMU to the ADV sensor-head and \vec{a}' is the high-pass filtered IMU acceleration.

After these motion correction steps are completed, instrument-frame velocity signals are rotated into the earth (inertial) frame using the IMU’s time-dependent orientation matrix. Finally, all velocity signals are rotated into a right-handed ‘prin-

cipal axes’ coordinate system such that u, x are aligned with the ebb-flood direction ($+u, +x$: ebb), v, y the cross-stream direction and $+w, +z$ the vertical-up direction. For the Admiralty Head and Nodule Point sites this corresponds to the $+u$ direction at $312^\circ T$ and $343^\circ T$, respectively (Figure 2).

2.2 Turbulence Statistics

The mean (\bar{u}) and turbulent (u') components of the stream-wise velocity are defined as,

$$u = \bar{u} + u' \quad . \quad (3)$$

Here the over-bar denotes a 5-minute average. Analogous expressions apply for the v and w components. The separation of mean-flow from turbulence at 5-minutes was chosen so that tidal variability can be considered negligible - and turbulence stationary - within a segment [10].

TKE spectra are computed using a fast Fourier transform (FFT or \mathcal{F}) of 5-minute detrended, hanning-windowed segments with 50% overlap, $S(u) = |\mathcal{F}(u')|^2$. Spectra are then grouped by mean velocity to obtain spectra with approximately 20 degrees of freedom. Spatial coherence (Γ) is estimated from two independent measurements of the same component of velocity (e.g. u_1 and u_2) that are separated in space by a distance $r = (\Delta x^2 + \Delta y^2 + \Delta z^2)^{1/2}$,

$$\Gamma(u) = \frac{|\overline{\mathcal{F}(u'_1) \mathcal{F}(u'_2)}|^2}{S(u_1) S(u_2)} \quad . \quad (4)$$

Here the over-bar denotes a 5-minute ensemble average of 128-second FFTs. The 95% confidence level of Γ measurements - above which Γ estimates can be considered valid with 95% confidence - is equal to $\sqrt{6/n_{DOF}}$, where n_{DOF} is the number of degrees of freedom in the coherence estimate [11].

3 RESULTS

3.1 Mean flow and Turbulent Velocity

The tidal velocity (streamwise) at the Admiralty Head is dominated by tidal harmonics (Figure 4A) and also possess non-harmonic variability (e.g. the second ebb of June 13th) that indicates the influence of topographic and other non-linear effects. Agreement between AWAC and moored ADV estimates of \bar{u} velocity demonstrates that moored IMU-ADV measurements can produce reliable estimates of this important inflow variable. Turbulence velocity fluctuations measured by the AWAC and ADV have similar amplitude, but peaks in the AWAC measurements are larger due to higher Doppler-noise and spatial aliasing.

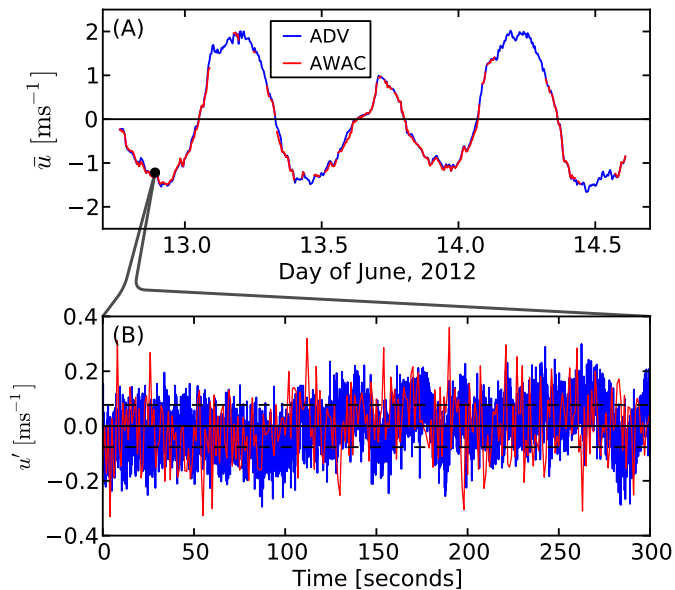


FIGURE 4. COMPARISON OF ADV (BLUE) AND AWAC (RED) VELOCITY (11m ABOVE THE BOTTOM). A) MEAN VELOCITY OVER THE 2-DAY ‘ADMIRALTY HEAD’ DEPLOYMENT, AWAC VELOCITY ESTIMATES ARE OMITTED WHERE THEY WERE CONTAMINATED BY SIDELobe REFLECTION FROM THE MOORING. B) TURBULENT VELOCITY FLUCTUATIONS FOR ONE 5-MINUTE SEGMENT (BLACK DOT IN A). HORIZONTAL DASHED LINES INDICATE ONE STANDARD DEVIATION OF THE ADV-MEASURED u' .

3.2 Turbulence spectra

Thomson et.al. 2013 showed that uncorrected TTM velocity estimates (\bar{u}_{ADV}) are affected by mooring motion (\bar{u}_m) particularly in the 0.1-1Hz frequency (f) band. This ‘motion-contamination’ can be removed so that, in agreement with turbulence theory, inertial frame TKE spectra reveal a $k^{-5/3}$ inertial-subrange (Figure 5). Here, k is wavenumber, and it can be converted to a proxy frequency f using Taylor’s ‘frozen field’ hypothesis, in which $f = \frac{\bar{u}k}{2\pi}$. At lower frequency ($f < 0.08\text{Hz}$), the observed spectral shape matches independent spectral estimates from fixed-frame ADV measurements ($S(\bar{u}_{\text{fixed}})$).

These methods can be used to produce accurate estimates of $S(u)$ - and $S(w)$ from moored ADVs equipped with IMUs (Figure 6B, blue and red). However, $S(v)$ is contaminated by motion that is too large to be completely removed (Figure 6B, green).

Inspection of the \vec{a} and $\vec{\omega}$ signals reveals that the 0.17Hz peak in the u_m and v_m spectra is due to swaying of the mooring line, and oscillations of the vane about the mooring-line axis. This frequency is consistent with oscillations induced by vortex shedding from the 37inch (0.94m) diameter spherical buoy [12].

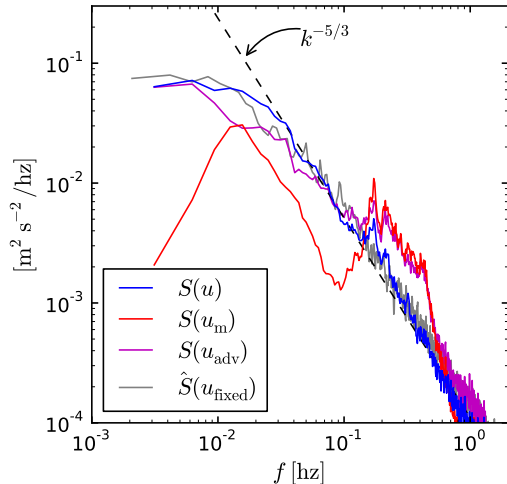


FIGURE 5. U-COMPONENT TURBULENCE SPECTRA OF MOORED ADV MEASUREMENTS FOR $\bar{u} = 1\text{m/s}$. A COMPARISON OF MOTION SPECTRA (RED) TO TURBULENCE SPECTRA BEFORE (PURPLE) AND AFTER (BLUE) MOTION CORRECTION. SPECTRA FROM A FIXED VELOCITY MEASUREMENT SCALED TO MATCH THE TOTAL TKE AND DISSIPATION OF THE MOORED SPECTRA IS PROVIDED FOR COMPARISON (GREY).

TKE spectra from the East River are higher energy than those at Admiralty Head. $S(u)$, in particular, is four-times larger at low-frequency (3e-3Hz) than the turbulence at Admiralty Head. Furthermore, the turbulent energy dissipation rate (estimated from the inertial sub-range, where $S(u) \propto k^{-5/3}$) is six-times larger than at Admiralty Head. It is likely that the higher turbulent energy at the RITE site is due to the measurements being closer to the bottom, bathymetric influences and flow-structure interactions (such as the bridge-abutment upstream of the RITE site).

3.3 Spatial Coherence

Estimates of $\Gamma(u)$ and $\Gamma(v)$ from ADVs on the TTM 10m above the seafloor have a similar dependence with f as cross-stream Γ measurements from a fixed-frame 4.6m above the riverbed in the East River (Figure 7). At both sites, Γ is high at low f and decays to zero near $f_r = \bar{u}/(2\pi r)$. These results agree with a turbulence-cascade theory that small scale fluctuations (high f) are less correlated than large scale fluctuations (low f). In particular, the theory that turbulence cascades to increasingly small eddies suggests that velocity fluctuations (eddies) should be uncorrelated over distances much larger than their size.

The Γ estimates at Admiralty Head (Figure 7A) were made from velocity measurements on a single vane of the TTM. This

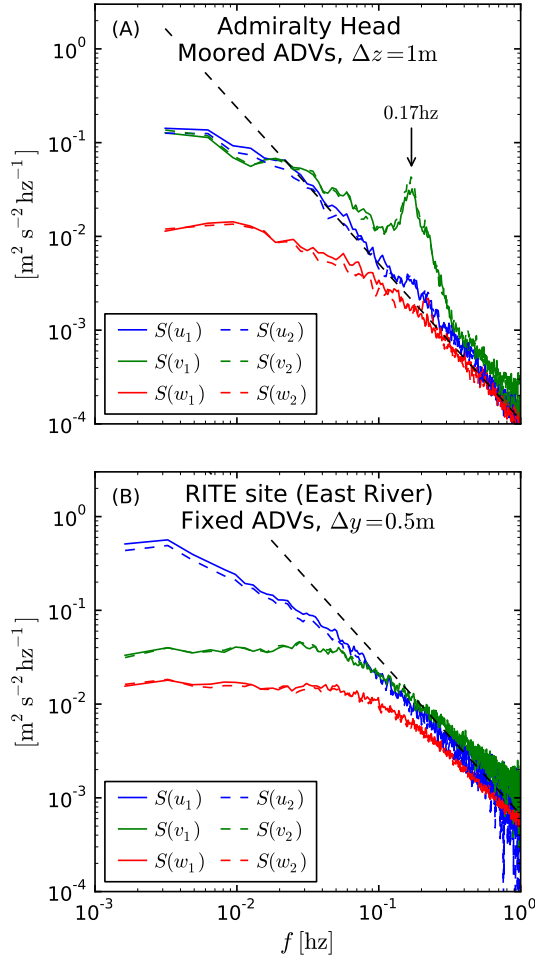


FIGURE 6. TKE SPECTRA FROM A COMPLIANT MOORING IN ADMIRALTY INLET (A), AND A RIGID TOWER IN THE EASTRIVER (B), FOR $|\bar{u}| = 1\text{ms}^{-1}$. A PAIR OF ADVS WERE DEPLOYED AT EACH SITE (I.E. MEASURED \bar{u}_1 AND \bar{u}_2); SPECTRA FROM BOTH INSTRUMENTS ARE SHOWN (DASHED VS. SOLID LINES). BLACK DASHED LINES INDICATE $k^{-5/3}$ SLOPES.

means that mooring motion that is not fully resolved by the IMU cannot be removed using (1), and this will leak into (contaminate) Γ estimates. This was the case for $\Gamma(v)$ (not shown). The two signals used to compute Γ are not fully-independent estimates of velocity. The instruments are on the same strongback-vane, and therefore motion not completely removed by (1) will elevate Γ . This issue is confounded by the fact that motion measurements were interpolated from one ADV to the other (section 2). Therefore, noise in those motion measurements will incorrectly increase Γ estimates.

Given these confounding factors, these mooring-based estimates of $\Gamma(u)$ and $\Gamma(w)$ are encouraging. If mooring motion can

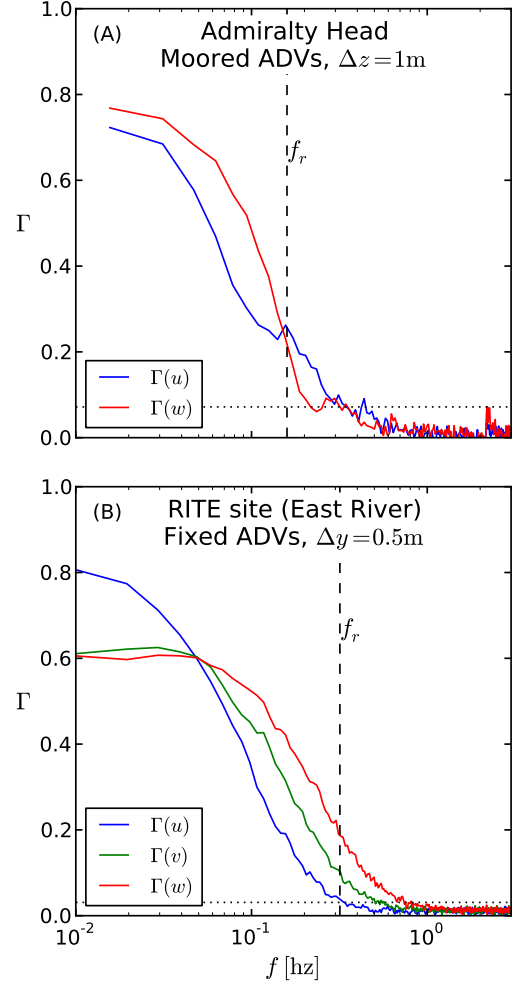


FIGURE 7. SPATIAL COHERENCE MEASUREMENTS FROM A COMPLIANT MOORING IN ADMIRALTY INLET (A) AND A RIGID TOWER IN THE EASTRIVER (B). DOTTED HORIZONTAL LINES INDICATE 95% CONFIDENCE LEVELS, AND VERTICAL DASHED LINES INDICATE THE SEPARATION FREQUENCY f_r OF THE MEASUREMENTS.

be reduced and fully independent IMU-ADVs are used it seems reasonable to expect that reliable Γ estimates can be made. If the low- f portion of the Γ estimates can be shown to be realistic, than empirical models of coherence could be used to interpolate over small motion-contamination peaks that persist [13].

3.4 Coherence Length

A length scale representative of the correlated velocity fluctuations (i.e. the predominant size of eddies that are correlated

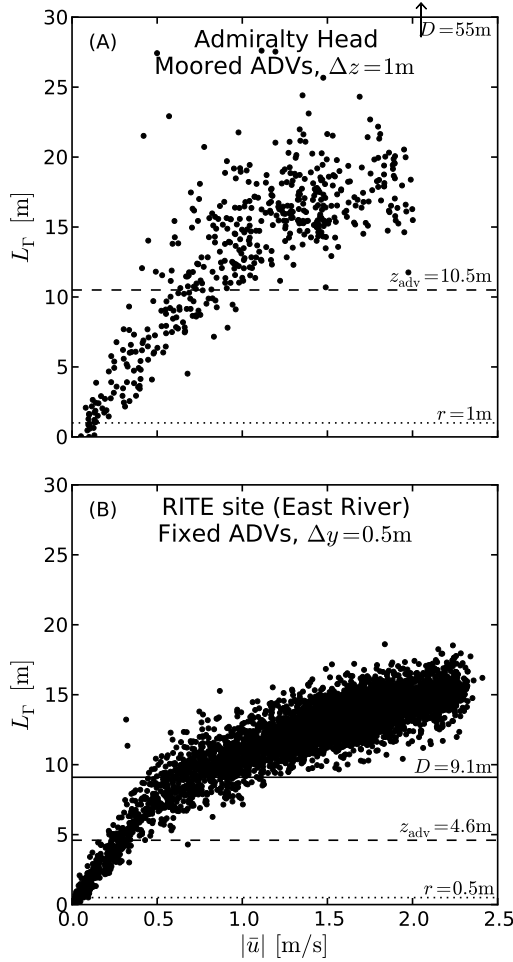


FIGURE 8. SPATIAL COHERENCE LENGTH L_Γ MEASURED AT THE ADMIRALTY HEAD SITE (A) AND THE RITE SITE (B).

over the measurement distance r) can be estimated as,

$$L_\Gamma = |\bar{u}| \frac{\int_0^\infty f^{-1} \Gamma df}{\int_0^\infty \Gamma df} \quad (5)$$

At both the Admiralty Head and RITE sites L_Γ increases linearly for $|\bar{u}| < 0.5$ (Figure 8). For $|\bar{u}| > 0.5\text{ms}^{-1}$, L_Γ appears to be limited by the external scales of the flow and measurements (i.e. the water depth, D , and height of measurements, z_{adv}). At the RITE site the slope of L_Γ with $|\bar{u}|$ decreases for $L_\Gamma > z_{\text{adv}}$, and is a distinctly smaller slope for $L_\Gamma \geq D$ (Figure 8B). Though it is less distinct (there is less data and the length scales are larger) this behavior appears to occur at the Admiralty Head site as well. These results indicate that coherence is determined by both the scales of the measurement (r and z_{adv}) and the external scales of the flow. This gives confidence that with more measurements of

Γ at MHK turbine sites models of that coherence based on these scales can be developed.

4 Conclusions

Fixed-tower ADV measurements provide reliable estimates of inflow conditions (including Γ) but are expensive to maintain and deploy in comparison to moorings, especially at hub heights greater than 5 m above the seabed. Furthermore, in order to fully characterize the inflow environment at tidal and river hydro-kinetic sites, coherence will need to be estimated at multiple spatial separations (e.g. $r = 0.5, 3, 15\text{m}$). This will necessitate multiple measurement platforms (towers or moorings) at additional cost.

Compliant moorings equipped with IMU-ADV (TTMs) offer significant promise for quantifying the turbulent inflow conditions at MHK turbine power sites. Already, reliable estimates of \bar{u} , \bar{w} , $S(u)$, $S(w)$ and $\Gamma(w)$ can be made from these platforms. Given this success, it is reasonable to expect that improvements in mooring design can reduce mooring motion so that \bar{v} , $S(v)$, $\Gamma(u)$ and $\Gamma(v)$ can also be measured more accurately. If this can be done, it will represent a significant step forward for tidal device site characterization and ocean measurement capability in general.

5 Future Work

To test whether moored ADV measurements can be used to estimate \bar{v} , $S(v)$ and all components of Γ a test-deployment of an improved mooring design will take place in June of 2014. In this experiment two TTMs will be deployed at the Admiralty Head site (Figure 2, yellow) in Admiralty Inlet (Puget Sound, WA). This site is well characterized, both in terms of power resource and turbulence statistics [4, 10]. The moorings will be configured similar to the original TTM. The primary components will be railroad wheel anchors, acoustic releases, instrument vanes with ADV mounts, and steel floats for buoyancy. Mooring components will be connected by spectra line, using a ‘fair-wrap’ to reduce strum and swivels to reduce twist loads. Faired cowlings will be added to the steel floats and ‘strongback vanes’ to reduce mooring motion. The moorings will be sub-surface with a maximum height of 15 m above the sea bed (40m below the surface). Each mooring will have at least two ADVs with integrated Microstrain IMUs configured for internal recording at 16Hz and synchronized with Network Time Protocol servers prior to deployment. The vertically separated, fully-independent velocity measurements from these instruments will be used to estimate vertical spatial coherence (Δz).

The two moorings will be deployed in two configurations. The first configuration will place the moorings laterally across the flow (Δy) and the second configuration will be streamwise (Δx) with the flow. For the lateral configuration, the separation

distance will be $\Delta y < 20m$ in order to capture correlated turbulence within the limiting length scale for isotropic turbulence (i.e., the depth, which is about 55 m). For the streamwise configuration, the separation distance may be expanded because advection by the mean flow should extend the effective coherent length scales. The default however, would be to use the same separation in both configurations. These separation distances will be refined during final planning. In addition to the two TTMs, an ADP will be deployed on a separate frame (to avoid mooring interference with ADP beams) near the TTMs to provide an independent estimate of the mean vertical velocity profile.

The results of the test-deployment will be published and data will be released publicly in early 2015. If this approach produces reliable estimates of Γ , a complete and detailed description of the methods will also be published so that future site-characterization studies can utilize moored ADVs to quantify the turbulent inflow at tidal-energy sites.

ACKNOWLEDGMENT

Thanks to Vincent Neary and Budi Gunawan for assisting with data processing of the East River dataset. Thanks to Joe Talbert, Alex deKlerk, and Capt. Andy Reay-Ellers for mooring engineering and deployment support. Also, thank you to Linux, Python, NumPy, Matplotlib, L^AT_EX and Emacs developers for creating the free software that facilitated efficient authoring and professional composition of this document.

REFERENCES

- [1] Moriarty, P. J., Holley, W. E., and Butterfield, S., 2002. “Effect of turbulence variation on extreme loads prediction for wind turbines”. *Transactions - American Society of Mechanical Engineers Journal of Solar Energy Engineering*, **124**(4), pp. 387–395.
- [2] Hand, M. M., Kelley, N. D., and Balas, M. J., 2003. Identification of wind turbine response to turbulent inflow structures. Tech. Rep. NREL/CP-500-33465, National Renewable Energy Laboratory, June.
- [3] Kelley, N. D., Jonkman, B. J., Scott, G. N., Bialasiewicz, J. T., and Redmond, L. S., 2005. The impact of coherent turbulence on wind turbine aeroelastic response and its simulation. Tech. Rep. NREL/CP-500-38074, National Renewable Energy Laboratory, August.
- [4] Thomson, J., Polagye, B., Durgesh, V., and Richmond, M., 2012. “Measurements of turbulence at two tidal energy sites in Puget Sound, WA”. *Journal of Oceanic Engineering*, **37**(3), pp. 363–374.
- [5] Stacey, M. T., Monismith, S. G., and Burau, J. R., 1999. “Measurements of reynolds stress profiles in unstratified tidal flow”. *J. Geophys. Res.*, **104**(C5), pp. 10933–10949.
- [6] Thomson, J., Kilcher, L., Richmond, M., Talbert, J., deKlerk, A., Polagye, B., Guerra, M., and Cienfuegos, R., 2013. “Tidal turbulence spectra from a compliant mooring”. In 1st Marine Energy Technology Symposium.
- [7] Finlayson, D., 2005. Combined bathymetry and topography of the Puget Lowlands, Washington state.
- [8] LORD MICROSTRAIN. *3DM-GX3-25 Miniature Attitude Heading Reference system product datasheet*.
- [9] Gunawan, B., Neary, V. S., and Colby, J., 2014. “Tidal energy site resource assessment in the East River tidal strait, near Roosevelt Island, New York, NY (USA).”. *Renewable Energy*. in press.
- [10] Polagye, B., and Thomson, J., 2013. “Tidal energy resource characterization: methodology and field study in admiralty inlet, Puget Sound, WA (USA)”. *Proceedings of the Institution of Mechanical Engineers, Part A: Journal of Power and Energy*, **227**(3), pp. 352–367.
- [11] Priestley, M., 1981. *Spectral Analysis and time series*. Academic Press.
- [12] Sakamoto, H., and Haniu, H., 1990. “A study on vortex shedding from spheres in a uniform flow”. *ASME Transactions Journal of Fluids Engineering*, **112**, Dec., pp. 386–392.
- [13] Thresher, R., Holley, W., Smith, C., Jafarey, N., and Lin, S., 1981. Modeling the response of wind turbines to atmospheric turbulence. Tech. rep., Oregon State Univ., Corvallis (USA). Dept. of Mechanical Engineering.